

LETTER TO THE EDITOR

TESS exoplanet candidates validated with HARPS archival data

A massive Neptune around GJ 143 and two Neptunes around HD 23472^{*}

Trifon Trifonov¹, Jan Rybizki¹, and Martin Kürster¹

Max-Planck-Institut für Astronomie, Königstuhl 17, D-69117 Heidelberg, Germany
e-mail: trifonov@mpia.de

Received xxx / Accepted xxx

ABSTRACT

Aims. We aim at the discovery of new planetary systems by exploiting the transit light curve results from TESS orbital observatory's Sector 1 and 2 observations and validating them with precise Doppler measurements obtained from archival HARPS data.

Methods. Taking advantage of the reported TESS transit events around GJ 143 (TOI 186) and HD 23472 (TOI 174) we model their HARPS precise Doppler measurements and derive orbital parameters for these two systems.

Results. For the GJ 143 system TESS has reported only a single transit, and thus its period is unconstrained from photometry. Our RV analysis of GJ 143 reveal the full Keplerian solution of the system, which is consistent with an eccentric planet with a mass almost twice that of Neptune and a period of $P_b = 35.59^{+0.01}_{-0.01}$ days. Our estimates of the GJ 143 b planet are fully consistent with the transit timing from TESS. We confirm the two-planet system around HD 23472, which according to our analysis is composed of two Neptune mass planets in a possible 5:3 MMR.

Key words. techniques: radial velocities – planets and satellites: detection – dynamical evolution and stability

1. Introduction

The Transiting Exoplanet Survey Satellite (TESS; Ricker et al. 2015) has begun its planet hunt. As of December 2018 the official TESS data release constitutes of a total of 54 days of TESS observations from Sectors 1 and 2 taken between 22 July and 21 September. Since then, a number of TESS planet candidates have been confirmed via ground based Doppler spectroscopy (Huang et al. 2018; Gandolfi et al. 2018; Wang et al. 2018; Jones et al. 2018), and given this high rate of planet detections one could easily predict a plethora of new planet discoveries during the 2-yr-mission. In this paper we report the Doppler validation of two additional TESS systems using archival HARPS spectra. We find an eccentric planet with almost two Neptune masses around the K dwarf GJ 143 (TOI 186), Its period of $P_b = 35.59^{+0.01}_{-0.01}$ d matches the single the transit timing event from TESS. We provide evidence of the existence of a two-planet system around HD 23472 (TOI 174) which is likely composed of two Neptune mass planets in a period ratio of 5:3 MMR.

This paper is organized as follows: in Section 2, we present estimates of the stellar parameters of GJ 143 and HD 23472, we present the available HARPS data and our approach to modeling the RV data. We present our results for these two exoplanet systems in Section 3 and in Section 4 we provide a brief summary and conclusions from this study.

Table 1. Stellar parameters with 1σ uncertainties for the planet hosts.

Parameters	GJ 143	HD 23472
Mass [M_\odot]	$0.76^{+0.03}_{-0.02}$	$0.75^{+0.04}_{-0.03}$
Radius [R_\odot]	0.73 ± 0.01	0.73 ± 0.01
Luminosity [L_\odot]	0.197 ± 0.003	0.231 ± 0.005

2. The GJ 143 and HD 23472 planet host candidates

We derive stellar parameters using the *isochrones* package (Morton 2015) together with the MIST stellar evolutionary tracks (Dotter 2016) assuming zero extinction. Input data are the BVJK bands taken from Simbad together with the Gaia DR2 parallaxes (which we correct for the zero point offset). The inferred parameters and their precision for the two K-dwarfs GJ 143 (≈ 39 pc) and HD 23472 (≈ 16 pc) are listed in Table 1. We neglect systematic uncertainties, but a test using a different isochrone set yielded very similar results.

2.1. HARPS data

The HARPS spectra of GJ 143 and HD 23472 were collected by our team prior to the TESS observations with an ultimate goal to re-analyze all publicly available ESO HARPS spectra in order to derive uniformly processed HARPS-Doppler measurements and study possible small but significant instrument related RV systematics (i.e., Tal-Or et al. 2018). We plan to make these data publicly available as a service to the exoplanet community (Trifonov et al. in prep.). All spectra in our MPIA HARPS-archive are reprocessed with the SERVAL (SpEctrum Radial Velocity Analyser, Zechmeister et al. 2018) pipeline, which is has been

^{*} Based on observations collected at the European Organization for Astronomical Research in the Southern Hemisphere under ESO programmes 072.C-0488, 183.C-0972, 183.C-0972, 085.C-0019, 087.C-0831, 089.C-0732, 089.C-0732, 090.C-0421

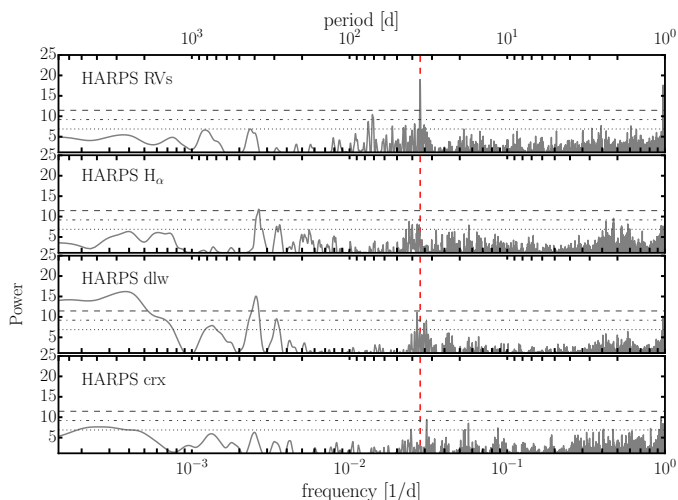


Fig. 1. Top: GLS periodogram of the SERVAL time series with levels of the false alarm probability (FAP) of 10% (dotted line), 1% (dot-dashed line) and 0.1% (dashed line). Second to fourth panel: Activity indicators following Zechmeister et al. (2018), H_α line index, differential line width (dLW), and chromatic index (CRX). The HARPS RVs clearly exhibit a significant peak at 35.6 d, which has no counterpart in the activity indices.

demonstrated to produce more precise RV measurements from HARPS spectra than the standard ESO HARPS-DRS pipeline (e.g. see Trifonov et al. 2018; Kaminski et al. 2018). In addition to the precise Doppler measurements we inspect the activity index measurements of the H_α line, the differential line width of the spectral lines and the RV chromaticity (wavelength dependence), respectively (for more details see Zechmeister et al. 2018).

GJ 143 has 54 HARPS measurements with a mean RV precision of 0.55 m s^{-1} taken between November 2003 and December 2009, plus four measurements with a mean RV precision of 1.26 m s^{-1} taken after the HARPS fiber upgrade (since May 2015, see Lo Curto et al. 2015) in the nights from 18 to 26 December 2016. It is well known that after this intervention HARPS is effectively a new instrument with a notable RV offset between the data taken before and after the fiber exchange. Lo Curto et al. (2015) have estimated that for a star of spectral type K such as GJ 143 the mutual RV offset is likely of the order of $10\text{--}12 \text{ m s}^{-1}$, which challenges the detection of low amplitude RV signals. Therefore, we decide to use the full HARPS data set of GJ 143, but as a standard practice in this case we model a mutual RV offset between the pre- and the post-upgrade RVs.

HD 23472 has only 14 precise HARPS RV measurements taken between February 2004 and February 2013 (all taken before the fiber upgrade). The mean precision of the RV data is 1.37 m s^{-1} , but the RV scatter is $\approx 13.5 \text{ m s}^{-1}$, which can be taken as a hint of the presence of planetary companions. Of course, such a scatter is not uncommon in stars with no obvious planet detections and the 14 RVs are not sufficient for a period search. Only after taking into account the *a priori* knowledge from the TESS transit periods and orbital phases is it possible to model these data for the presence of planet companions.

2.2. RV modeling

To derive the best-fit model of the RV data we adopt a Maximum Likelihood Estimator (MLE) scheme coupled with a Nelder-

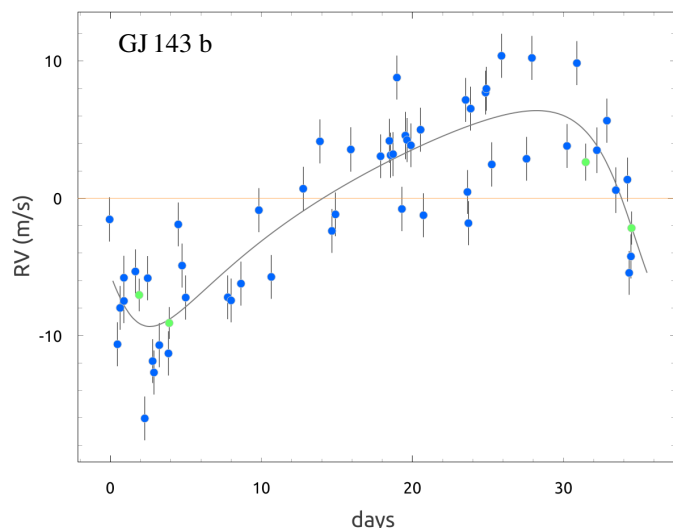


Fig. 2. HARPS RV data phased to the best-fit period of $P_b = 35.589 \text{ d}$. Blue data are the pre-fiber upgrade data, while green data are post-fiber upgrade data. After fitting for the mutual RV offset these data sets are consistent with each other. The orbital solution is consistent with the TESS transit event. The RV uncertainties include the estimated RV jitter, which was quadratically added to the error budget.

Mead algorithm (Nelder & Mead 1965), which optimizes the likelihood function ($-\ln \mathcal{L}$) of a Keplerian or an N-body model. We model the standard the RV curve parameters such a semi-amplitude K , period P , eccentricity e and arguments of periastron ω . Instead of the time of periastron passage t_p we model the planetary mean anomalies M for a given epoch, which is more convenient parameter in the case of an N-body model, which yields osculating orbital parameters of a given epoch. In our study the GJ 143, and HD 23472 mean anomalies are defined at the first HARPS observational epoch for each data set. In addition to these parameters we follow the methodology of Baluev (2009) and we add the unknown RV variance (RV jitter) as an additional parameter.

We analyze the parameter distributions and estimate parameter uncertainties by coupling our MLE fitting code to a Markov Chain Monte Carlo (MCMC) sampling scheme using the *emcee* sampler (Foreman-Mackey et al. 2013). More details about our fitting tools, including a GUI interface can be found in <https://github.com/3fon3fonov/trifon> (Trifonov et al. in prep.).

3. Results

3.1. GJ 143

The official TESS Sector 1 & 2 data release has not provided a transit period of the GJ 143 candidate companion. This is because only a single but significant transit of GJ 143 has been observed between 22 July to 21 September for this target. Thus from the transit alone we have no prior knowledge of the period, but the RV data together with the mid-time of the detected transit can in principle reveal the planetary parameters.

Figure 1 shows a Generalized Lomb-Scargle periodogram (GLS; Zechmeister & Kürster 2009) of the SERVAL time series products of the GJ 143 HARPS spectra. The RV measurements exhibit a strong peak at 35.62 d with a significant GLS power of 0.6721 marking our planetary candidate. There is no significant

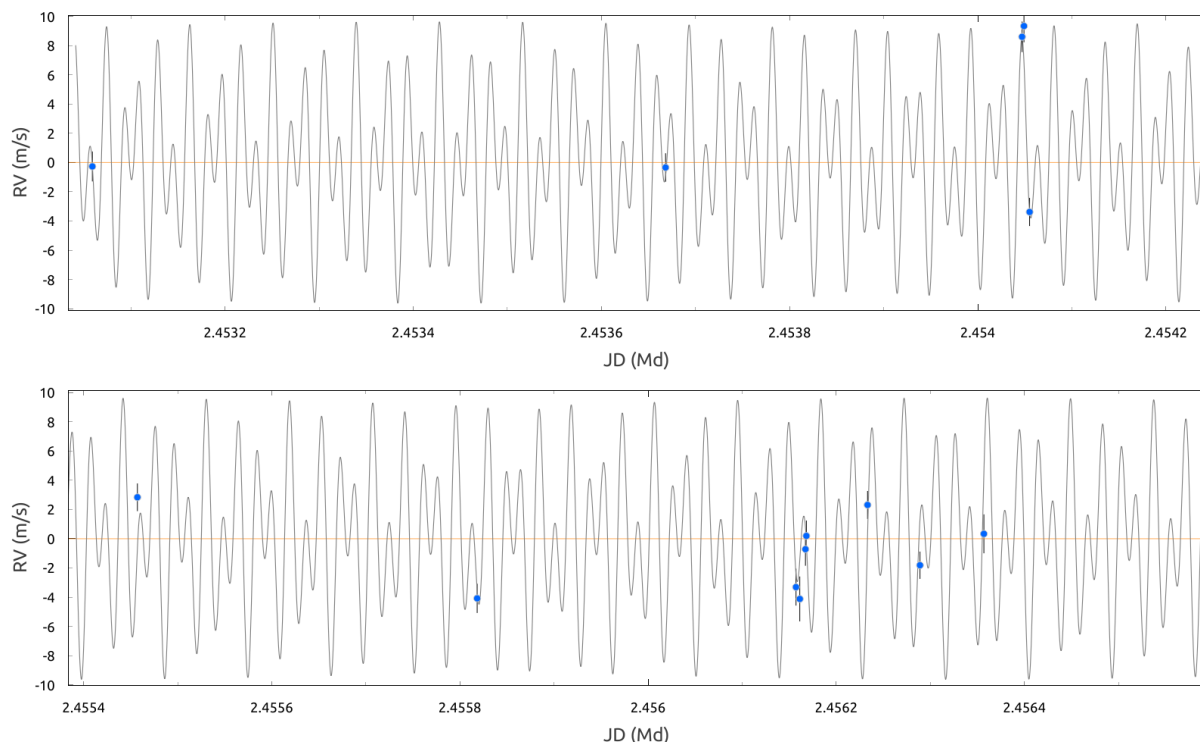


Fig. 3. Doppler data time series of GJ 143 obtained with HARPS. The small number of data points (14) is not by itself sufficient to discover the planets, but taking advantage of the *a priori* knowledge of the TESS transit ephemerides, makes it possible to construct a two-planet model, which is in excellent agreement with the RV data (see Table 2 for details). As in Fig. 2 the RV uncertainties include the RV jitter.

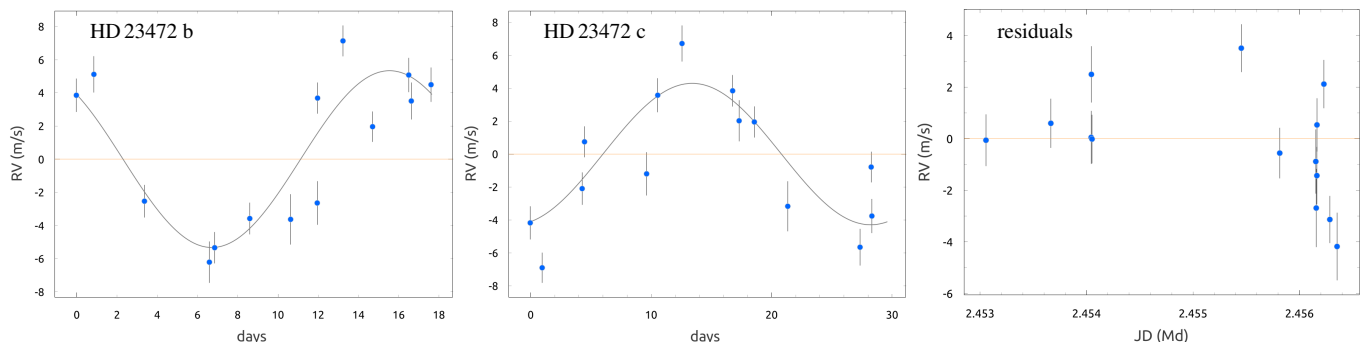


Fig. 4. Same model and data for GJ 143 as in Fig. 3, but folded to the best circular periods for each planet. Shown from left to right are the phase folded RVs pertaining to planets HD 23472 b and c and the residuals from the model.

power at this period in the HARPS-SERVAL activity indicators. It is worth noting that the measurements of the differential line width activity indicator display significant excess power at very small frequencies and at a period of ≈ 400 d, the latter confirmed by the H_α index. This may mean that GJ 143 is a somewhat active star.

Given the strong indication of a planet-induced signal we apply a full Keplerian model to the RV data. However, while we were sampling around the best-fit model, we rejected all the confident MCMC samples whose configurations would not lead to a transit event at BJD = 2458350.312 with a tolerance of ± 2 h. We converged to a best-fit solution consistent with a planet with a mass of $30.6 M_\oplus$ (almost twice the mass of Neptune) orbiting with a period of $P_b = 35.6$ d on a moderately eccentric orbit with $e_b = 0.33$. Orbital parameter estimates and MCMC uncertainties for GJ 143 b are provided in Table 2. The best-fit solution and

its confidence region are fully consistent with the transit event reported by TESS.

3.2. HD 23472

The two transiting exoplanet candidates around HD 23472 inferred from TESS observations have periods of $P_b = 17.6800 \pm 0.0015$ d and $P_c = 29.8102 \pm 0.0047$ d, respectively. The durations of both transits are $\approx 3 \pm 0.3$ h, leading to estimated planetary radii consistent with Neptune-sized objects, $R_b = 1.872 \pm 1.321 R_\oplus$ and $R_c = 2.149 \pm 0.345 R_\oplus$, respectively. To measure the most likely masses of the planetary candidates we model the available HARPS data using a two-planet circular Keplerian model, and use as a prior the transit information. In this case, the only unconstrained parameters in this model are the RV semi-amplitudes $K_{b,c}$ (related to the planetary masses), since

Table 2. Keplerian parameters of GJ 143 b and a two-planet circular configuration of HD 23472 based on HARPS archival RV measurements.

Orb. param.	One-planet Keplerian	Two-planet Keplerian with circular orbits	
	GJ 143 b	HD 23472 b	HD 23472 c
K [m s ⁻¹]	7.60 ^{+0.64} _{-0.65}	5.33 ^{+0.67} _{-4.20}	4.29 ^{+0.26} _{-3.44}
P [d]	35.589 ^{+0.006} _{-0.005}	17.667 ^{+0.142} _{-0.095}	29.625 ^{+0.224} _{-0.171}
e	0.325 ^{+0.079} _{-0.079}	0.0 (fixed)	0.0 (fixed)
ϖ [deg]	121.8 ^{+19.2} _{-19.1}	0.0 (fixed)	0.0 (fixed)
M [deg]	10.2 ^{+14.5} _{-14.4}	42.9 ^{+260.3} _{-35.5}	196.7 ^{+107.3} _{-79.0}
a [au]	0.1932 ^{+0.0002} _{-0.0002}	0.121 ^{+0.001} _{-0.001}	0.170 ^{+0.001} _{-0.001}
m_p [M_\oplus]	30.63 ^{+2.63} _{-2.67}	17.92 ^{+1.41} _{-14.00}	17.18 ^{+1.07} _{-13.77}

the transit epoch and periods are well established by the photometry. However, we decided to include the planetary periods and phases in the modeling. Our reason for this is the following: Over the ≈ 14 years of RV measurements small deviations of the oscillating orbit may accumulate to strong deviations from an unperturbed sine-like curve in some phases where RV data is obtained. Moreover, albeit precise, there is only a limited number of TESS transits (perhaps only two for HD 23472 c) and thus we do not know the scale of the gravitational interaction in the system, which may have a strong impact on the orbital perturbation and transit timing variations (TTVs). We note that taking the exact period estimates from TESS leads to a very poor fit and thus allowing the planetary periods to be adjusted slightly in the modeling is well justified. Our best-fit circular model is shown in Fig. 3 and Fig. 4, while Table 2 summarizes its parameters and MCMC uncertainties. We find very consistent estimates of HD 23471 b whose period is very close to that found by TESS, whereas for HD 23471 c the period deviates by about 4 h which, however, is still within the MCMC-derived errors.

For completeness, we also tested a full two-planet dynamical model, which led to a marginally better fit. This fit suggests a somewhat eccentric inner planet with $e_b = 0.2$, and the dynamical integration of this configuration revealed a much larger oscillation of the period ratio of P_c/P_b from 1.64 to 1.70 with a mean period of 1.67, hence in a potential 5:3 mean motion resonance (MMR). Fig. 5 shows the N-body evolution of the P_c/P_b of the two-planet circular and the full dynamical models within the baseline of the observations (using SyMBA; Duncan et al. 1998). Clearly, both configurations are dynamically active, which shows how challenging the multiplanet modeling of sparse archival data could be due to the unknown magnitude of the dynamical perturbations in the system. Albeit that the full N-body model is more realistic and may to some extent explain the small deviation of the period of HD 23472 c, when compared with the TESS results, modeling those sparse 14 HARPS RVs with such a complex model is not justified. Therefore, we limit our dynamical analysis of the HD 23472 system to an initially circular solution (i.e. fixed $e_{b,c} = 0$, $\omega_{b,c} = 0$), which is already a good model.

We alert that more RV data may be needed to set firm constraints to the orbital parameters and dynamical masses of the HD 23472 system. This can be effectively done by modeling the transit photometry and RVs simultaneously when more data is collected. Until then the ambiguity in the models continues to exist, although the magnitude of the HD 23472 b and c planetary masses is already determined in the range of few Earth masses to

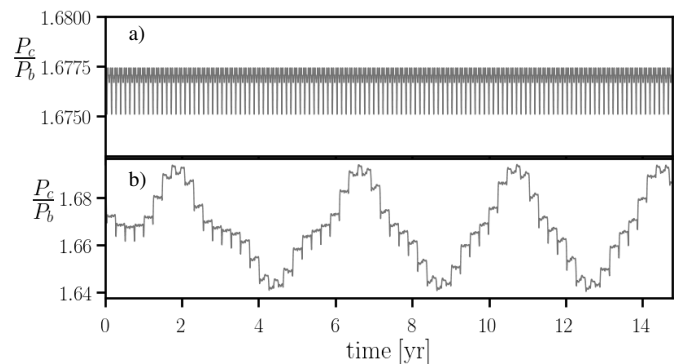


Fig. 5. Numerical integration of the HD 23472 system between the first HARPS data epoch and the TESS transit event epoch on the inner planet. Panel a) shows the evolution of the two-planet circular fit tabulated in Table 2. Panel b) shows the evolution of a full dynamical model to the HARPS data, which is consistent with moderately eccentric inner planet at start ($e_{\text{bint.}} = 0.2$) and thus stronger orbital oscillations. The mean period ratio in both cases, is slightly above 5:3, which may hint at a resonant system.

more likely Neptune mass planets, which was our scientific goal with this paper.

4. Conclusions

We report the confirmation of two new planetary systems discovered with TESS. GJ 143 system is an interesting case because, given the orbital period of the GJ 143 companion, TESS was capable to detect only a single transit, and thus no reported period was available. However, the RV data of GJ 143, together with the transit constraints from TESS reveal an eccentric massive Neptune with $30.6^{+2.7}_{-2.6} M_\oplus$ and a period of $P_b = 35.59^{+0.01}_{-0.01}$ d. We provide strong arguments for a two-planet system around HD 23472, which is likely composed of two Neptune-mass planets with $17.9^{+1.4}_{-14.0} M_\oplus$ and $17.2^{+1.1}_{-13.8} M_\oplus$, respectively. The two planets are consistent with a period ratio of 5:3, which may indicate a second-order MMR system.

GJ 143 would benefit from more photometric data to fully constrain the transit period and the system configuration in general. Similarly, HD 23472 would benefit from more RV measurements, which together with the transit photometry could lead to a more conclusive dynamical analysis revealing the exact planetary masses and possible resonant motion involved.

We validate the existence of these two TESS planetary system candidates by using HARPS archival data taken prior to the TESS observations. This shows the importance of archival Doppler data in the TESS era.

Acknowledgements. JR was funded by the DLR (German space agency) via grant 50 QG 1403. This research has made use of the SIMBAD database, operated at CDS, Strasbourg, France. This work has made use of data from the European Space Agency (ESA) mission *Gaia* (<https://www.cosmos.esa.int/gaia>), processed by the *Gaia* Data Processing and Analysis Consortium (DPAC, <https://www.cosmos.esa.int/web/gaia/dpac/consortium>). Funding for the DPAC has been provided by national institutions, in particular the institutions participating in the *Gaia* Multilateral Agreement. This paper includes data collected by the TESS mission. Funding for the TESS mission is provided by the NASA Explorer Program. We are extremely grateful to all the people behind the TESS mission and light curves for making this science possible.

References

- Baluev, R. V. 2009, MNRAS, 393, 969
- Dotter, A. 2016, ApJS, 222, 8
- Duncan, M. J., Levison, H. F., & Lee, M. H. 1998, AJ, 116, 2067
- Foreman-Mackey, D., Hogg, D. W., Lang, D., & Goodman, J. 2013, PASP, 125, 306
- Gandolfi, D., Barragán, O., Livingston, J. H., et al. 2018, A&A, 619, L10
- Huang, C. X., Burt, J., Vanderburg, A., et al. 2018, arXiv e-prints [arXiv:1809.05967]
- Jones, M. I., Brahm, R., Espinoza, N., et al. 2018, arXiv e-prints [arXiv:1811.05518]
- Kaminski, A., Trifonov, T., Caballero, J. A., et al. 2018, A&A, 618, A115
- Lo Curto, G., Pepe, F., Avila, G., et al. 2015, The Messenger, 162, 9
- Morton, T. D. 2015, isochrones: Stellar model grid package, Astrophysics Source Code Library
- Nelder, J. A. & Mead, R. 1965, Computer Journal, 7, 308
- Ricker, G. R., Winn, J. N., Vanderspek, R., et al. 2015, Journal of Astronomical Telescopes, Instruments, and Systems, 1, 014003
- Tal-Or, L., Trifonov, T., Zucker, S., Mazeh, T., & Zechmeister, M. 2018, ArXiv e-prints [arXiv:1810.02986]
- Trifonov, T., Kürster, M., Zechmeister, M., et al. 2018, A&A, 609, A117
- Wang, S., Jones, M., Shporer, A., et al. 2018, arXiv e-prints [arXiv:1810.02341]
- Zechmeister, M. & Kürster, M. 2009, A&A, 496, 577
- Zechmeister, M., Reiners, A., Amado, P. J., et al. 2018, A&A, 609, A12

Table A1. HARPS Doppler and activity index measurements of GJ 143

Epoch [JD]	RV [m s ⁻¹]	σ_{RV} [m s ⁻¹]	H α	$\sigma_{H\alpha}$	dLW	σ_{dLW}	CRX [m s ⁻¹]	σ_{CRX} [m s ⁻¹]
2452944.721	9.696	0.636	0.5941	0.0005	-5.9561	1.0546	-9.6681	4.9699
2452999.632	10.457	0.658	0.5941	0.0007	-25.7717	1.2432	-7.7947	5.3430
2453229.926	3.251	0.412	0.6004	0.0005	-17.0397	0.8972	-3.0486	3.3220
2453269.827	4.006	0.593	0.6031	0.0008	-5.0468	1.4548	7.1507	4.7088
2453272.829	3.794	0.400	0.5990	0.0005	-19.8159	1.0137	7.3744	3.0630
2453668.802	11.932	0.466	0.5992	0.0006	-24.3391	1.0298	2.6644	3.6875
2453765.524	-0.626	0.416	0.5928	0.0004	-32.9353	1.3126	9.0655	3.1110
2453786.575	17.766	0.479	0.5940	0.0005	-24.9761	1.1744	3.3407	3.7635
2453787.561	18.933	0.408	0.5960	0.0005	-24.1359	1.1263	4.0667	3.1895
2453974.883	5.803	0.471	0.6020	0.0006	-12.8689	0.9478	-4.5192	3.7062
2453980.853	6.334	0.500	0.6007	0.0005	-12.8008	1.0412	0.2311	3.9921
2453983.878	4.021	0.387	0.5963	0.0004	-20.5988	0.9191	0.5757	3.0842
2454047.702	0.602	0.508	0.5935	0.0005	-32.0755	1.0400	10.3017	3.7750
2454049.705	5.416	0.599	0.5908	0.0005	-25.9886	0.8742	1.3131	4.7498
2454051.726	9.332	0.398	0.5951	0.0005	-19.9435	0.8746	5.0952	3.0866
2454083.692	5.446	0.462	0.5993	0.0005	-26.9660	0.9060	8.0434	3.5204
2454120.634	-4.799	0.419	0.5950	0.0006	-4.7482	2.3679	3.8152	3.2804
2454121.598	0.538	0.602	0.5911	0.0006	-29.1790	1.0787	1.7083	4.7521
2454314.887	14.450	0.514	0.5977	0.0007	3.6912	0.9118	6.6093	4.0270
2454316.899	10.000	0.507	0.6050	0.0005	0.3611	0.7384	-5.1915	4.0138
2454319.876	9.423	0.543	0.6086	0.0006	-7.8703	1.0424	-7.0581	4.2600
2454528.522	20.029	0.497	0.6038	0.0004	-6.1047	0.6842	2.0576	3.9910
2454705.921	14.373	0.880	0.6037	0.0011	10.6964	1.6758	1.0048	7.0407
2454706.899	15.805	1.366	0.6039	0.0015	18.6017	1.9954	-0.2727	10.8934
2454707.903	16.230	0.515	0.6044	0.0006	3.3062	1.0135	-6.1598	4.0988
2454710.887	18.400	0.490	0.6100	0.0006	4.2387	1.0656	-2.1125	3.9769
2454732.763	10.370	0.534	0.6014	0.0006	-14.0461	0.9638	10.1990	4.1314
2454736.806	15.380	0.508	0.6017	0.0006	8.3691	0.9711	2.8532	4.0894
2454738.849	14.792	0.681	0.6016	0.0010	14.9087	1.6128	7.9205	5.3517
2455025.910	15.420	0.531	0.6035	0.0006	28.8658	1.4241	3.8046	4.2451
2455040.898	11.827	1.017	0.6159	0.0011	44.0798	1.8401	-19.4108	7.7271
2455041.897	7.001	0.586	0.6039	0.0006	34.5170	1.2768	-18.8928	3.9624
2455043.900	3.755	0.655	0.5990	0.0008	24.3797	1.1110	-16.3918	4.8049
2455045.888	-1.456	0.559	0.5999	0.0006	8.9963	1.0172	2.0762	4.4753
2455046.847	-0.064	0.615	0.5972	0.0006	3.6089	1.0721	-5.1147	4.8809
2455067.891	19.211	0.484	0.6003	0.0004	13.4789	1.1128	2.2069	3.8953
2455068.893	21.614	0.556	0.6120	0.0006	20.5423	1.2959	-3.2975	4.4146
2455070.906	21.460	0.500	0.6067	0.0005	30.7554	1.5415	3.7429	3.9604
2455073.884	21.082	0.497	0.6040	0.0005	42.4130	1.5426	-2.3507	3.9240
2455075.872	16.889	0.579	0.6100	0.0006	48.9282	1.8006	-17.8538	3.9402
2455103.812	13.701	0.632	0.6010	0.0008	17.8320	1.3525	-1.8507	5.0376
2455108.791	15.046	0.449	0.6054	0.0006	19.5356	1.2438	3.0267	3.5510
2455110.770	14.735	1.013	0.6040	0.0013	37.5307	1.9733	7.0893	8.0616
2455112.790	12.597	0.506	0.6030	0.0005	24.8694	1.1726	-7.4645	3.8934
2455115.784	5.904	0.589	0.6098	0.0006	25.6761	1.2292	-12.2261	4.4087
2455122.775	5.019	0.521	0.6040	0.0006	0.1916	0.9857	-8.9392	3.9827
2455124.781	5.507	0.412	0.5976	0.0004	-4.6902	0.7896	0.9842	3.3344
2455128.793	8.857	0.472	0.5993	0.0005	-11.9238	0.8935	-0.9934	3.7745
2455133.765	15.478	0.541	0.5924	0.0006	2.9067	0.9629	-1.5358	4.3192
2455137.765	11.695	0.408	0.5981	0.0004	0.2423	0.8599	-8.0442	3.1099
2455141.675	14.112	0.403	0.5943	0.0005	-0.6146	0.8849	-0.4292	3.2072
2455164.591	10.064	0.375	0.6032	0.0004	4.2105	0.7454	-3.3703	2.9801
2455167.579	14.297	0.365	0.5965	0.0004	-1.9728	0.8741	-5.0357	2.8736
2455169.584	15.096	0.357	0.5911	0.0004	0.7791	0.9048	-5.7168	2.7619
★ 2457741.707	26.049	1.700	0.5965	0.0004	10.5170	4.1623	22.7319	14.0814
★ 2457744.742	21.247	1.208	0.6001	0.0004	20.5421	3.9814	0.6533	10.3213
★ 2457747.712	16.371	1.137	0.6036	0.0004	27.4149	3.7602	4.3749	9.6055
★ 2457749.702	14.332	1.010	0.6073	0.0005	26.8128	4.3433	2.3767	10.0253

Notes. ★ – HARPS Doppler measurements taken after the fibre upgrade (May 2015; see [Lo Curto et al. 2015](#), and text for details).

Table A2. HARPS Doppler and activity index measurements of GJ 143

Epoch [JD]	RV [m s ⁻¹]	σ_{RV} [m s ⁻¹]	H α	$\sigma_{H\alpha}$	dLW	σ_{dLW}	CRX [m s ⁻¹]	σ_{CRX} [m s ⁻¹]
2453059.535	2.873	1.201	0.5519	0.0016	-2.4184	1.2866	-5.3629	9.9618
2453668.823	2.802	1.028	0.5615	0.0013	-2.3712	0.8061	-0.5300	8.1486
2454047.724	11.741	1.285	0.5642	0.0016	5.5847	1.1331	4.5335	10.0359
2454049.740	12.478	1.478	0.5656	0.0016	3.1887	1.2196	11.4607	11.5097
2454055.743	-0.242	0.984	0.5661	0.0015	1.0254	1.1512	2.1167	7.7627
2455457.786	5.974	0.931	0.5613	0.0013	2.5872	0.9143	6.0835	7.3470
2455818.918	-0.941	1.125	0.5600	0.0013	1.2704	0.8332	-15.6541	8.7661
2456157.811	-0.172	1.898	0.5602	0.0019	2.2810	1.3152	6.3535	15.0879
2456161.850	-0.981	2.565	0.5711	0.0035	7.7206	2.8759	17.9903	20.5379
2456167.849	2.422	1.534	0.5586	0.0017	0.7274	1.2243	11.6636	12.1493
2456168.831	3.332	1.298	0.5604	0.0015	0.4062	1.0128	-8.0084	10.2524
2456233.856	5.450	0.963	0.5651	0.0014	3.4175	0.8908	-9.5777	7.5427
2456289.590	1.325	0.872	0.5600	0.0010	-5.2491	0.5648	-6.2508	6.8533
2456357.506	3.474	2.069	0.5689	0.0022	2.1101	1.6997	10.6605	16.6006